Contents lists available at ScienceDirect

Veterinary Microbiology

journal homepage: www.elsevier.com/locate/vetmic

Short communication

Identification and characterization of PEDV infection in rat crypt epithelial cells

Jianing Chen, Yaru Cui, Zemei Wang, Guangliang Liu *

State Key Laboratory of Veterinary Etiological Biology, Lanzhou Veterinary Research Institute, Chinese Academy of Agricultural Sciences, Lanzhou, Gansu 730046, China

A B S T R A C T

Porcine epidemic diarrhea (PED) is a devastating enteric disease to the world's swine production. Porcine epidemic diarrhea virus (PEDV), as the PED causative agent, has been commonly propagated and investigated in Vero cells, as well as in IPEC-J2, a porcine epithelial cell-jejunum 2. However, Vero cells, which are defective in interferon production, cannot represent the host response in enteric cells while PEDV replicates poorly in IPEC-J2 cells. In this study, we observed that rat crypt epithelial cells (IEC-6) were highly susceptible to different subtypes of PEDV. The replication kinetics of PEDV in IEC-6 cells is similar to that in Vero cells, but it is much higher than in IPEC-J2 cells. Besides that, PEDV infection in IEC-6 cells can induce the production of inflammatory cytokines and interferon, especially the type III IFNs. Collectively, our findings suggest that IEC-6 is an ideal cell line for PEDV replication and immune response studies.

1. Introduction

The swine enteric coronaviruses, a family of the most significant problematic pathogens to the world's swine industry, include porcine epidemic diarrhea virus (PEDV), porcine transmissible gastroenteritis virus (TGEV), porcine deltacoronavirus (PDCoV), and swine acute diarrhea syndrome coronavirus (SADS-CoV) (Qiuhong et al., 2019). Among these four viruses, PEDV has been recognized as the most devastating pathogen, causing up to 100 % mortality in piglets younger than one week old. Since its first discovery in the 1970s, PEDV has then subsequently identified nearly worldwide (Wood, 1977). Later in the 2010s, variant PEDV strains were emerged and killed hundreds of millions of suckling piglets (Jung and Saif, 2015; Wang et al., 2016).

PEDV is an enveloped, single-stranded, positive-sense RNA virus, which targets the small intestine, especially the ileum (Lee, 2015). PEDV infection in enterocytes can exhibit acute necrosis, leading to marked villous atrophy in the small intestine (Ducatelle et al., 1982). Consequently, malabsorption, caused by the massive loss of absorptive enterocytes, contributes to diarrhea and even death of newborn piglets. The cell line, which is permissive for PEDV replication and possesses the intestine function and responses, may facilitate the studies about PEDV. Vero cells are commonly used for PEDV propagation. However, this cell line is characterized by lacking the production of interferon (Desmyter

et al., 1968). Consequently, it is valuable in vaccine production but defective in immune studies. IPEC-J2 is a non-transformed porcine columnar epithelial cell line and used in the investigations of PEDV (Chen et al., 2019; Lin et al., 2017). However, it is semi-permissive to PEDV infection and defective in the production of several cytokines (Brosnahan and Brown, 2012). These drawbacks of the two cell lines restrict further understandings of PEDV. Therefore, it is of great importance to screen proper cell lines for PEDV investigations.

In this study, we identified rat crypt epithelial cells (IEC-6) was highly susceptible to a different subtype of PEDV, which could be an ideal cell model for PEDV studies.

2. Materials and methods

2.1. Cells and viruses

The rat small intestine epithelium IEC-6 cells were purchased from American Type Culture Collection (ATCC) and cultured in Dulbecco's modified Eagle's medium (DMEM) (Sigma, Germany) supplemented with 0.1 Unit/ml bovine insulin and 10% fetal bovine serum (Gemini, USA). African green monkey epithelial Vero cells were cultured in DMEM medium supplemented with 10% fetal bovine serum. The intestinal porcine epithelial cell line J2 (IPEC-J2) cells were cultured in

---

Table 1
The primer sets used for RT-PCR and real-time qPCR analysis.

Gene	Genus	Forward primer	Reverse primer
NSP12	PEDV	GGCTTATTTAAACGAGTACGGGGCT	TTGTAAAACTGCAGATTTCTCATA
	Porcine	CAGTTCTGCACTGGACTGGA	CACAGGGGCTGTAGCTCTTC
IFN-α	Rat	CTGTCCTGCATGAGCTGACC	GGAGATTCCTGCACCCCTAC
	Chlorocebus sabaeus	CAGAGACTCCCCTGATGAACAA	CCAGGCACAAAGGCTGTATTTC
	Porcine	TGCAACCACCACAATTCC	CTGAGAATGCCGAAGATCTG
IFN-β	Rat	ACTTGGGTGACATCCACGAC	AAGACTTCTGCTCGGACCAC
	Chlorocebus sabaeus	GAGCCGTAGTGGAGAAGCAC	GGCCATACCCATCTAACTGC
	Porcine	GCCATTCAAAGGAGCATGGAT	CTGATGGCTTTGCGCTGGAT
IFN-γ	Rat	CATCGCCAAGTTCGAGGTGA	TCTGGTGACAGCTGGTGAATC
	Chlorocebus sabaeus	TGAATGTCCAACGCAAAGCA	TCGACCTCGAAACATCTGACT
	Porcine	TGGCCTTAGAGGCTGAGCTA	CCCTGATGCAAGCCTGAAGT
IFN-λ1	Rat	GGCCAAGGATGCCATTGAAG	GGGTCAGTCATGTTCCCCAA
	Chlorocebus sabaeus	AATCTCTGTCACCGCAAGAGT	TCACCTGGAGAAGCCTTAGGT
IFN-λ3	Porcine	GTCCCTCTTGGAGGACTGGA	TGCTGTGCAGGGATGAGTTC
	Rat	GGCCAAGGATGCCATTGAAG	TGGGTCAGTCATGTTCCCCA
	Porcine	GGCCATAGTACCTGAACCCG	CCAAGGTCCAGGTTTTGGGT
IL-1β	Rat	GATGAGGACCCAAGCACCTT	GTCGTCATCATCCCACGAGT
	Chlorocebus sabaeus	GTGGCAACGAGGATGACTTG	GCCCTTGTTGTAGTGCTCGT
	Porcine	AATGCTCTTCACCTCTCC	TCACACTTCTCTATACTTCTCA
IL-6	Rat	AGAGACTTCCAGCCAGTTGC	AGTCTCCTCTCCGGACTTGT
	Chlorocebus sabaeus	TTCGGTCCAGTTGCCTTCTC	CTGAAGAGGTCAGTGGCTGG
	Porcine	CTGAGAGTGATTGAGAGT	TTACTGCTGTTGTTGTTG
IL-8	Rat	CTCCAAACCTTTCCACCCCA	TTCCTTGGGGTCCAGACAGA
	Chlorocebus sabaeus	GTGGACCACACTGCGTCAAT	CTCCACAACCCTAGACACCC
	Porcine	AAGTCCAGGATGCCCAAA	CGGTTCAAGATGTTCAAGTTG
IL-17A	Rat	CTGAGGGGAAGTTGGACCAC	TAGAGGAAACGCAGGTGCAG
	Chlorocebus sabaeus	AACCGGAATACCAATACCAGTCTC	CTCTCAGGGTCCTCATTGCG
	Porcine	GTCTCAAACCTCAGATAAG	GTTGTCTTTCAGCTTCAC
TNF−α	Rat	TCGTAGCAAACCACCAAGCA	GTGAGGAGCACATAGTCGGG
	Chlorocebus sabaeus	CCTGGTATGAGCCCATCTACCTA	AGTCGGGCAGATTGATCTCAG
	Porcine	CAAGAAGGTGGTGAAGCAGG	ACCAGGAAATGAGCTTGACG
GAPDH	Rat	GCCATCAACGACCCCTTCAT	AGATGGTGATGGGTTTCCCG
	Chlorocebus sabaeus	AAATCAAGTGGGGCGATGCT	ACAAACATAGGGGCGTCAGC

DMEM/F12 (Sigma, Germany) supplemented with 10% fetal bovine serum, 5 μg/ml insulin/selenium/transferrin (Life, USA) and 5 ng/ml epidermal growth factors (EGF) (Life, USA). The PEDV LJX01/GS/2014 strain was isolated and conserved in our laboratory. The PEDV CV777 strain was isolated from attenuated vaccine and maintained in our laboratory.

2.2. Immunofluorescence assay

IEC-6 cells were seeded in 48-well plates. When grown to 80% confluency, cells were infected with PEDV at a MOI = 0.01. After 48 hours, the cells were fixed with 4% paraformaldehyde for 30 min and then permeabilized with 0.5% Triton X-100 for 15 min at room temperature. After blocking with 5% skim milk for 1 h, cells were incubated with mouse anti-PEDV-nucleocapsid monoclonal antibody (1:5000 dilution) for 1 h, followed by incubating with the Alexa Fluor 488 goat anti-mouse IgG antibody (1:1000 dilution) (Thermo, USA) for 1 h. The cell nuclei were stained by DAPI (Beyotime, China). The cells were then examined under a fluorescence microscope (TE2000U; Nikon) with a video documentation system.

2.3. Infection of different cells with PEDV

To assess the host response against PEDV, the three cell lines were infected with PEDV at a MOI = 0.01. The supernatant was collected at 12, 24, 36, 48, 60 and 72 hours post-infection and used for viral titration. At 24 hours post-infection, the cells were also lysed with TRIzol (Takara, Japan) for RNA extraction.

2.4. Plaque assay

Confluent monolayers of IEC-6 cells in 6-well plates were inoculated with PEDV and incubated for 1 h at room temperature on rocker. After three washes, the cells were overlaid with 0.75% low melting point agarose (Sigma, Germany) in DMEM containing 5% FBS and then incubated at 37℃ for around 72 h. To visualize plaques, cells were stained with 1% crystal violet in ethanol.

2.5. PEDV titration

Vero cells were seeded into 96-well plates and cultured for 80-90% confluence. The cell monolayers were washed three times with PBS. Serial 10-fold dilutions of the collected supernatant were made, and 100 μl of each dilution were inoculated to five wells of the 96-well plate. The plates were incubated at 37 °C and supplied with 5% CO_2. And then, the cultures were checked under a light microscope for cytopathology every day for 3 days. The dilution of the supernatant was titrated by $TCID_{50}$ assay and calculated based on the Reed-Muench method.

2.6. Real-time PCR analysis

For the detection of host gene expression level, the real-time qPCR was performed with unique aptamer qPCR SYBR green master mix (Novogen, China) in the Bio-Rad CFX96 system. The reactions were incubated at 94 °C for 30 s, followed by 45 cycles at 94 °C for 5 s and 60 °C for 30 s. All reactions were run in triplicate using the primer sets listed in Table 1. The $2^{-\Delta\Delta Ct}$ method was employed to measure the expression level of target genes.

2.7. Statistical analysis

The Student's *t*-test was used for the examination of statistical significance between matched groups. An unadjusted *P* value of less than 0.05 was considered significant; a *P* value of less than 0.01 was considered highly significant.
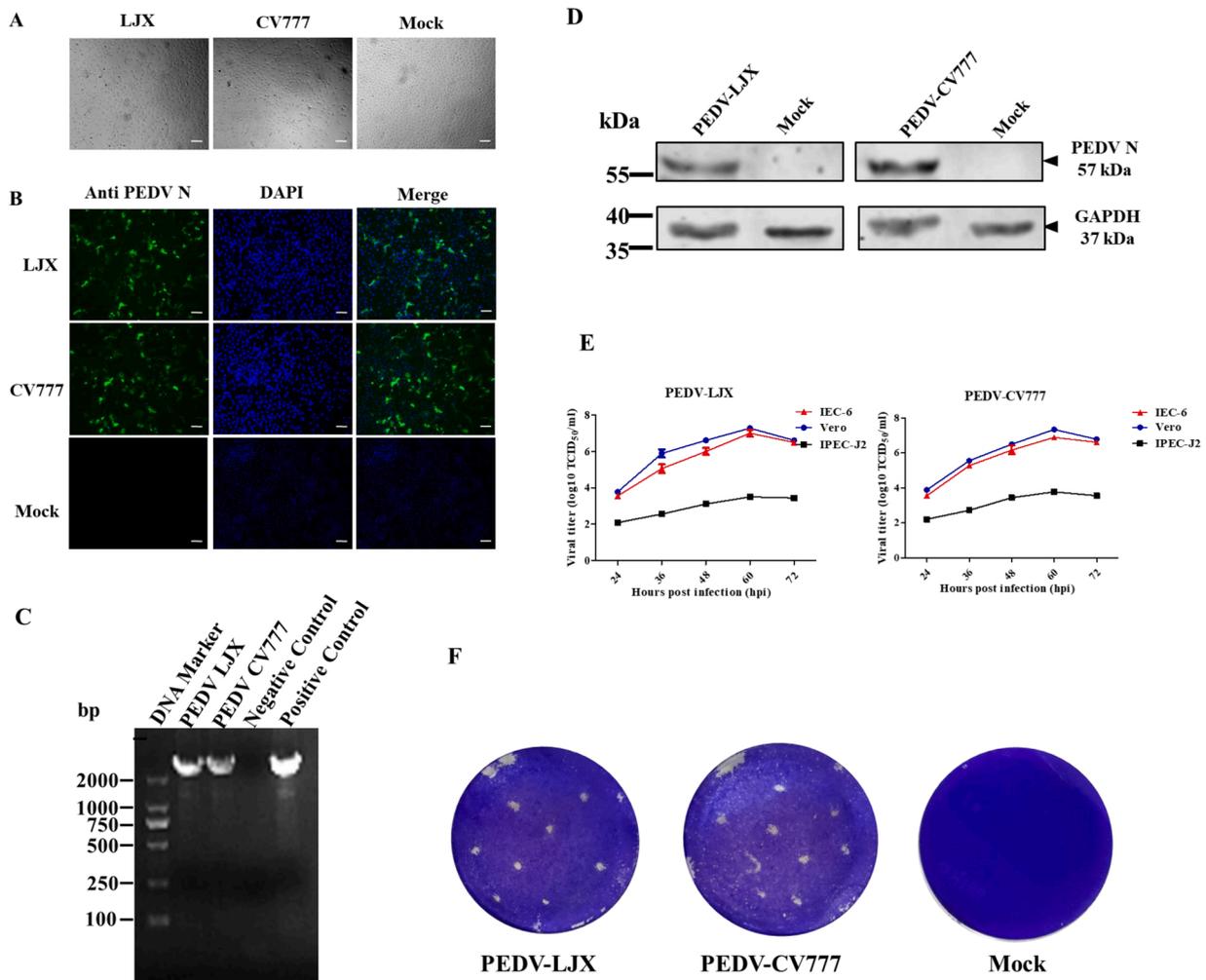
Fig. 1. IEC-6 cells were susceptible to different strains of PEDV. (A) Cytopathic effect of the infected and mock-infected IEC-6 cells. (B) Immunofluorescence staining of the infected and mock-infected IEC-6 cells. (C) RT-PCR detection of PEDV NSP12 gene in IEC-6 cells. (D) Western blot assay of PEDV N protein in IEC-6 cells infected with different strains of PEDV and mock-infected cells. (E) The growth curves of PEDV LJX and CV777 strains in IEC-6, IPEC-J2, and Vero cells. (F) The plaque assay of PEDV LJX and CV777 strains in IEC-6 cells. Magnification: $10 \times$. Scale bar = 100 μm.

3. Results

3.1. PEDV can infect IEC-6 cells

IEC-6 cell line, originally derived from the rat small intestinal crypt, was commonly used in the nutritional investigations (Quaroni et al., 1979). To investigate if it is susceptible to PEDV, the IEC-6 cells were infected with two different subtypes of PEDV at a MOI = 0.01 and observed for cytopathic effect (CPE) under a microscope. The PEDV vaccine strain CV777 belongs to subtype G1, while the field strain LJX isolated by our group belongs to subtype G2 (Guo et al., 2018). As shown in Fig. 1A, typical CPE became visible at 24 hours post-infection. The morphology of PEDV-infected cells became enlarged fusiform at early stage. Lately, they were wrinkled and detached. However, the mock-infected cells remained normal during the whole process. IFA was then performed to confirm its infection by using a mAb against PEDV nucleocapsid protein (Yang et al., 2019). The results showed that strong PEDV-N positive signals were observed in IEC-6 cells infected with either LJX strain or CV777 strain (Fig. 1B), indicating IEC-6 cells were successfully infected by PEDV. Then the total RNA was extracted and analyzed by RT-PCR. The results demonstrated that the PEDV-specific bands were amplified from virus-inoculated cells (Fig. 1C). Finally, the western blotting analysis showed that the PEDV nucleocapsid protein was detected in cells infected with PEDV (Fig. 1D). We also attempted to

identify whether the IEC-6 were susceptible to TGEV but no positive signal were obtained (data not shown). Taken together, the above data illustrated that IEC-6 cells were susceptible to PEDV but not TGEV.

Vero and IPEC-J2 cell lines were commonly used for PEDV investigation. To test and compare the replicative capacity of PEDV in different cell lines, the PEDV replication kinetics were measured in these three cell lines. These cells were seeded in the 24-well plate and inoculated with PEDV LJX strain or CV777 strain at a MOI = 0.01. The supernatant was collected every 12 hours and used for viral titration. The results showed that the PEDV LJX strain replicated poorly in IPEC-J2 cells with viral titers lower than 10^4 TCID$_{50}$/ml. PEDV LJX strain exhibited a robust and similar growth curve in Vero and IEC-6 cells, showing higher than 10^7 TCID$_{50}$/ml viral titers. PEDV CV777 strain reached its most elevated viral titers in both Vero and IEC-6 cells but poorly replicated in IPEC-J2 cells (Fig. 1E). The plaque assay is usually employed for virus purification and titration. It is of great importance to virus related studies. We also tested whether IEC-6 could be used to conduct plaque assay. The data showed that the infection of both LJX and CV777 strains resulted to the formation of plaque (Fig. 1F). These results further showed that IEC-6 cells supported PEDV infection and replication.

3.2. PEDV infection induces stable host immune responses in IEC-6 cells

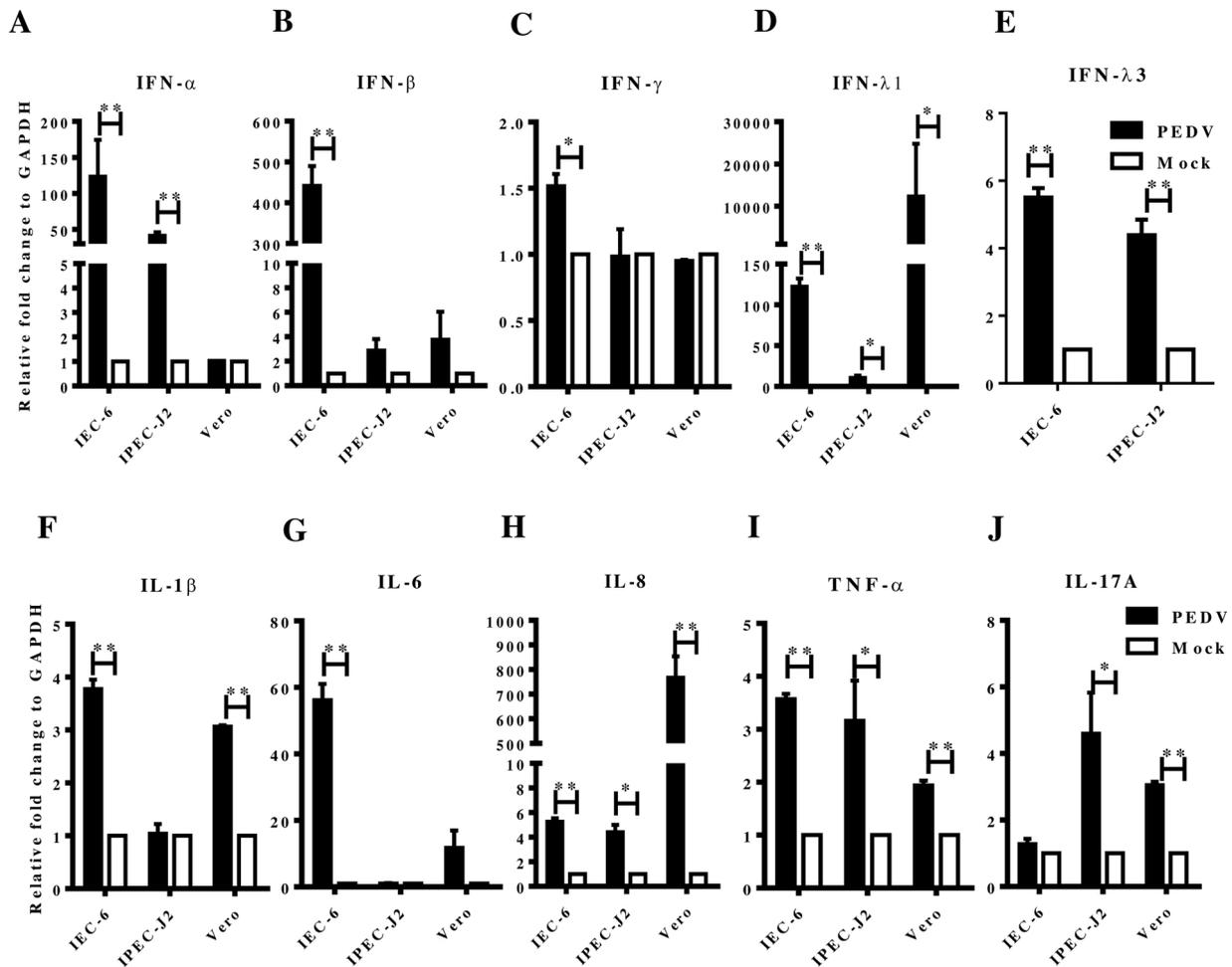PEDV infection in the porcine small intestine is characterized by

Fig. 2. The host immune response to PEDV LJX01/GS/2014 infection in different cell lines. The RT-qPCR analysis of (A) IFN-α, (B) IFN-β, (C) IFN-γ, (D) IFN-λ1, (E) IFN-λ3, (F) IL-1β, (G) IL-6, (H) IL-8, (I) IL-17A, and (J) TNF-α in different cell lines infected with PEDV LJX01/GS/2014 strain.

inflammatory cytokines and interferon (Jung and Saif, 2015). The type III interferon is considered to play a critical role in enteric immunity. Therefore, we examined whether PEDV infection could induce the typical enteric immunity in IEC-6 cells compared to its infection in IPEC-J2 and Vero cells. PEDV LJX was a field strain and was used to infect the three cell lines. After 24 hours post-infection, the RNA was extracted for RT-qPCR analysis. The results showed that both type I and type III interferon responses were significantly activated in PEDV infected IEC-6 and IPEC-J2 cells while the type I interferon were absent in Vero cells (Fig. 2A, B, D, E). Due to the lack of IFN-λ3 gene of green monkey in the NCBI or ENSEMBL database, we failed to detect its gene expression level. Although the IFN-λ3 gene of green monkey was strongly upregulated in PEDV infected Vero cells, its Ct value was about 30, while the Ct value to GAPDH was about 18 in PEDV infected cells. In mock cells, the Ct values of about 39 for IFN-λ3 and 18 for GAPDH. For type II interferon, PEDV infection led to a significant upregulation in IEC-6 cells but not in IPEC-J2 and Vero cells (Fig. 2C). PEDV infection also enhanced the expression of IL-1β, IL-6, IL-8, and TNFα in IEC-6 cells except for IL-17A (Fig. 2F, G, H, I, J). All these results demonstrated that IEC-6 cells were able to generate a robust immune response against PEDV infection.

4. Discussion

Although Vero and IPEC-J2 were commonly used in PEDV studies, they were defective in immune response and viral replication. There were also other cell lines identified permissive for PEDV infection

recently. PEDV can also infect HEK293, IP2-2I cells, and primary bovine mesenchymal cells (Jung et al., 2020; Wang et al., 2019; Zhang et al., 2017). However, HEK293 is not an intestinal epithelium cell line, while IPI-2I is semi-permissive to PEDV infection. The primary bovine mesenchymal cells cannot culture for a long time. The rat small intestinal crypt epithelium cell line IEC-6 is non-transformed. And it was often used as a necrotizing enterocolitis model system and nutritional studies (Braga-Neto et al., 2012; Ruthig and Meckling-Gill, 1999; Yan et al., 2018). The uptake, metabolism, and transport processes are observed in IEC-6 cells (Said et al., 1997; Sanderson and He, 1994). Therefore, IEC-6 is recognized as an ideal model for intestine relating studies. However, it is rarely used in viral studies. Only modified vaccinia virus Ankara was reported to multiply in IEC-6 cells (Okeke et al., 2006). In this study, we tested the susceptibility of IEC-6 cells to PEDV infection and found it was highly susceptible. The growth curve of PEDV in IEC-6 was similar to it in Vero cells with the viral titers higher than 10^7 $TCID_{50}$/ml. It was also found that IEC-6 could mimic the antiviral immune response in the small intestine. PEDV infection in the small intestine is characterized by the induction of proinflammatory responses (Huan et al., 2017). In our study, IL-1b, IL-6, IL-8, and TNFα were upregulated by PEDV infection in IEC-6 cells. Only TNFα, IL-17A and IL-8 were found increasingly expressed in IPEC-J2 cells. IL-6 was only activated by PEDV infection in IEC-6 cells. Besides that, interferon is recognized to play critical roles in the innate immune response. The type III interferon is significantly essential in maintaining intestinal homeostasis, especially to PEDV (Ingle et al., 2018; Zhang et al., 2018). In PEDV infected IEC-6 cells, the expression of type I and type III

interferon was drastically upregulated, while type II interferon was also increasingly expressed. Vero cells are defective in interferon production. The Ct values of all genes were higher than 29 while it was about 20 for GAPDH. Although IFN-λ1 was highly upregulated in Vero cells, its Ct value was also higher than 29. In IPEC-J2 cells, the production of IFNα, IFN-λ1, and IFN-λ3 was increased but not as high as in IEC-6 cells. All these data suggested that PEDV infection in IEC-6 cells could induce strong antiviral responses.

5. Conclusion

In summary, our studies identified the rat small intestinal crypt epithelium IEC-6 cells were highly susceptible to PEDV. PEDV could efficiently replicate in IEC-6 cells as it does in Vero cells. Besides that, PEDV infection activated potent inflammatory cytokines and interferon, primarily type III interferon in IEC-6 cells, which highly simulated its infection in the small intestine. All these data above suggested that IEC-6 cells can be used as an excellent cell model for PEDV studies.

Acknowledgments

Appendix A. Supplementary data

Supplementary material related to this article can be found, in the online version, at doi:https://doi.org/10.1016/j.vetmic.2020.108848.

References

Braga-Neto, M.B., Oliveira, B.M., Rodrigues, R.S., Noronha, F.J., Leitao, R.F., Brito, G.A., Lima, A.A., Guerrant, R.L., Warren, C.A., 2012. Protective effects of alanyl-glutamine supplementation against nelfinavir-induced epithelial impairment in IEC-6 cells and in mouse intestinal mucosa. Cancer Biol. Ther. 13, 1482–1490.

Brosnahan, A.J., Brown, D.R., 2012. Porcine IPEC-J2 intestinal epithelial cells in microbiological investigations. Vet. Microbiol. 156, 229–237.

Chen, J., Zhang, C., Zhang, N., Liu, G., 2019. Porcine endemic diarrhea virus infection regulates long noncoding RNA expression. Virology 527, 89–97.

Desmyter, J., Melnick, J.L., Rawls, W.E., 1968. Defectiveness of Interferon Production and of Rubella Virus Interference in a Line of African Green Monkey Kidney Cells (Vero). J. Virol. 2, 955–961.

Ducatelle, R., Coussement, W., Debouck, P., Hoorens, J., 1982. Pathology of Experimental CV777 Coronavirus Enteritis in Piglets. II. Electron Microscopic Study. Vet. Pathol. 19, 57–66.

Guo, J., Fang, L., Xu, Y., Chen, J., Xu, S., Zhu, X., Miao, Y., Dang, W., Xiao, S., 2018. Evolutionary and genotypic analyses of global porcine epidemic diarrhea virus strains. Transbound. Emerg. Dis.

Huan, C.C., Wang, H.X., Sheng, X.X., Wang, R., Wang, X., Mao, X., 2017. Glycyrrhizin inhibits porcine epidemic diarrhea virus infection and attenuates the proinflammatory responses by inhibition of high mobility group box-1 protein. Arch. Virol. 162, 1467–1476.

Ingle, H., Peterson, S.T., Baldridge, M.T., 2018. Distinct Effects of Type I and III Interferons on Enteric. Viruses 10.

Jung, K., Saif, L.J., 2015. Porcine epidemic diarrhea virus infection: Etiology, epidemiology, pathogenesis and immunoprophylaxis. Vet. J. (London, England : 1997) 204, 134–143.

Jung, K., Vasquez-Lee, M., Saif, L.J., 2020. Replicative capacity of porcine deltacoronavirus and porcine epidemic diarrhea virus in primary bovine mesenchymal cells. Vet. Microbiol. 244, 108660.

Lee, C., 2015. Porcine epidemic diarrhea virus: An emerging and re-emerging epizootic swine virus. Virol. J. 12, 193.

Lin, H., Li, B., Chen, L., Ma, Z., He, K., Fan, H., 2017. Differential Protein Analysis of IPEC-J2 Cells Infected with Porcine Epidemic Diarrhea Virus Pandemic and Classical Strains Elucidates the Pathogenesis of Infection. J. Proteome Res. 16, 2113–2120.

Okeke, M.I., Nilssen, O., Traavik, T., 2006. Modified vaccinia virus Ankara multiplies in rat IEC-6 cells and limited production of mature virions occurs in other mammalian cell lines. J. Gen. Virol. 87, 21–27.

Qiuhong, Wang, Anastasia, Vlasova, Scott, Kenney, Linda, 2019. Emerging and re-emerging coronaviruses in pigs. Curr. Opin. Virol.

Quaroni, A., Wands, J., Trelstad, R.L., Isselbacher, K.J., 1979. Epithelioid cell cultures from rat small intestine. Characterization by morphologic and immunologic criteria. J. Cell Biol. 80, 248–265.

Ruthig, D.J., Meckling-Gill, K.A., 1999. Both (n-3) and (n-6) fatty acids stimulate wound healing in the rat intestinal epithelial cell line, IEC-6. J. Nutr. 129, 1791–1798.

Said, H.M., Ma, T.Y., Ortiz, A., Tapia, A., Valerio, C.K., 1997. Intracellular regulation of intestinal folate uptake: studies with cultured IEC-6 epithelial cells. Am. J. Physiol. 272, C729–736.

Sanderson, I.R., He, Y., 1994. Nucleotide uptake and metabolism by intestinal epithelial cells. J. Nutr. 124, 131s–137s.

Wang, D., Fang, L., Xiao, S., 2016. Porcine epidemic diarrhea in China. Virus Res. 226, 7–13.

Wang, X., Fang, L., Liu, S., Ke, W., Wang, D., Peng, G., Xiao, S., 2019. Susceptibility of porcine IPI-2I intestinal epithelial cells to infection with swine enteric coronaviruses. Vet. Microbiol. 233, 21–27.

Wood, E.N., 1977. An apparently new syndrome of porcine epidemic diarrhoea. Vet. Rec. 100, 243–244.

Yan, J.K., Yan, W.H., Cai, W., 2018. Fish oil-derived lipid emulsion induces RIP1-dependent and caspase 8-licensed necroptosis in IEC-6 cells through overproduction of reactive oxygen species. Lipids Health Dis. 17, 148.

Yang, W., Chen, W., Huang, J., Jin, L., Zhou, Y., Chen, J., Zhang, N., Wu, D., Sun, E., Liu, G., 2019. Generation, identification, and functional analysis of monoclonal antibodies against porcine epidemic diarrhea virus nucleocapsid. Appl. Microbiol. Biotechnol. 103, 3705–3714.

Zhang, J., Guo, L., Xu, Y., Yang, L., Shi, H., Feng, L., Wang, Y., 2017. Characterization of porcine epidemic diarrhea virus infectivity in human embryonic kidney cells. Arch. Virol. 162, 2415–2419.

Zhang, Q., Ke, H., Blikslager, A., Fujita, T., Yoo, D., 2018. Type III Interferon Restriction by Porcine Epidemic Diarrhea Virus and the Role of Viral Protein nsp1 in IRF1 Signaling. Appl. Microbiol. Biotechnol. 92.